research papers

The NaCl- to CsCl-type phase transition discussed on the basis of the *cP* to *cI* deformation with the symmetry *Cmcm* 4(*c*) *m2m*

H. Sowa

Hahn-Meitner-Institut, Bereich Strukturforschung NE, Glienicker Strasse 100, D-14109 Berlin, Germany. Correspondence e-mail: heidrun.sowa@t-online.de

A structure forming a cubic primitive lattice *cP* may be deformed into a structure forming a cubic body-centred lattice *cI* in the space group *Cmcm* at position 4(*c*) *m2m* $0, y, \frac{1}{4}$. If in related structures the sites are alternately occupied by unlike atoms, the NaCl and the CsCl types occur, respectively. The corresponding phase transition can be described as a deformation of a heterogeneous sphere packing in the subgroup *Pmmn* ($\mathbf{a}, -\mathbf{c}, \mathbf{b}$) of *Cmcm*. All sphere configurations with symmetry *Cmcm* 4(*c*) *m2m* were derived. On the basis of this information, further possibilities for phase transitions that also correspond to sphere-packing deformations were found with this symmetry. Two of them possibly may take place in metals. The first one leads from a primitive hexagonal lattice to a hexagonal close packing, the other from a cubic body-centred lattice also to a hexagonal close packing.

1. Introduction

Phase transformations between NaCl-type and CsCl-type structures have been observed in many alkali halides and alkaline-earth oxides under high pressure while a reverse transition occurs in CsCl at high temperatures. Such a transition is accompanied by a change of the coordination number of all atoms from six in the NaCl type to eight in the CsCl type. These transitions have been extensively examined during the last decades. However, despite the many investigations, the transition mechanism that leads from the NaCl type to the CsCl type has not been thoroughly clarified. For the description of such a phase transition, two models are mainly discussed. The first one was proposed by Shoji (1931) and later modified by Buerger (1951) who showed that a contraction along one of the body diagonals of the unit cell of the NaCl structure type and an expansion normal to it result in the CsCl-type structure. This model is usually presented in standard texts. It implies that one of the $\langle 111 \rangle$ directions of the NaCl-type unit cell is parallel to one of the $\langle 111 \rangle$ directions of the CsCl-type cell. Another model was introduced by Watanabe *et al.* (1977) who investigated the CsCl- to NaCl-type phase transition in CsCl that occurs at high temperatures. These authors did not observe the orientation relation mentioned above but found that $[110]_{\text{CsCl}}$ is parallel to $[100]_{\text{NaCl}}$ and $[001]_{\text{CsCl}}$ is parallel to $[011]_{\text{NaCl}}$. They described the phase transition as an interlayer translational movement of atomic planes associated with an intralayer rearrangement of the atoms. The atoms within the (110) layers of the CsCl-type rearrange while half of these layers are shifted parallel to
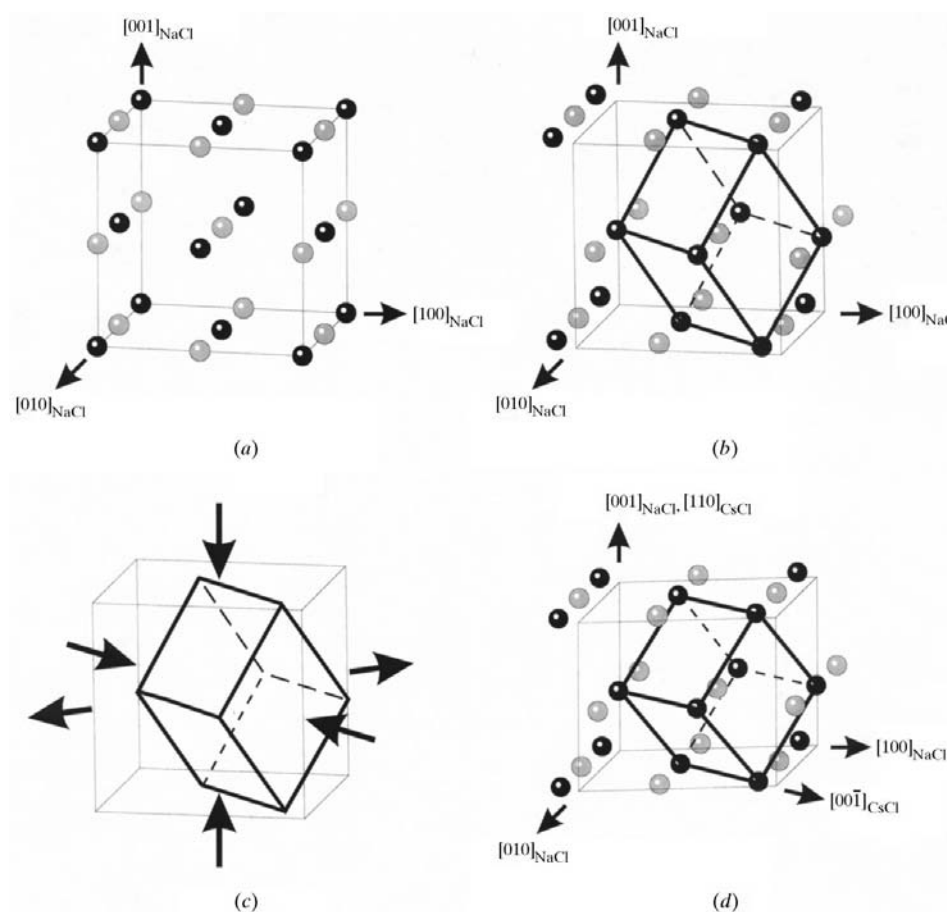
the [001] direction of the CsCl type. Perpendicular to the $(110)_{\text{CsCl}}$ planes, an elongation of the unit cell was observed. This transition model is usually attributed to Watanabe *et al.* (1977), but, as has already been stated by Kennedy (1980), such a mechanism exactly corresponds to the one that was described before by Hyde & O'Keeffe (1973).

In contrast to the transition in CsCl at high temperature, single crystals of alkali halides were destroyed during the pressure-induced phase transitions between the two structure types and orientation relations had to be determined by measuring the preferred orientation of the resulting powder. The relative orientations of the unit cells of the low- and high-pressure phases of alkali halides have been studied by several authors. Blaschko *et al.* (1979) obtained orientation relations from a high-pressure neutron-diffraction study of RbI analogous to those of Watanabe *et al.* (1977), while, for the same compound, Okai (1980) found the relations $[111]_{\text{CsCl}} \parallel [100]_{\text{NaCl}}$ and $[100]_{\text{CsCl}} \parallel [111]_{\text{NaCl}}$ using X-ray diffraction photography. Later, Okai (1981) investigated all rubidium and potassium halides with the exception of RbF and found the above relations for all these compounds. The results of Fujiwara *et al.* (1983) obtained on RbCl under high pressure with X-ray diffraction techniques agreed with those of Okai (1981). However, Onodera *et al.* (1992) observed the relations $[110]_{\text{CsCl}} \parallel [112]_{\text{NaCl}}$ and $[001]_{\text{CsCl}} \parallel [111]_{\text{NaCl}}$ also studying RbCl but using neutron diffraction. Ruff *et al.* (1989) performed molecular dynamics simulations of the polymorphic phase transitions in alkali halides. These calculations yielded the relations $[\frac{11}{22}\bar{1}]_{\text{CsCl}} \parallel [\bar{1}01]_{\text{NaCl}}$, $[110]_{\text{CsCl}} \parallel [010]_{\text{NaCl}}$ and $[111]_{\text{CsCl}} \parallel [001]_{\text{NaCl}}$. The different orientation relations in

the same compounds observed by several authors were attributed to different external conditions such as pressure or temperature or to the sample size (Fujiwara *et al.*, 1983). Onodera *et al.* (1992) perceived that a single transition mechanism may result in multiple orientation relations and stated that those derived from their study on RbCl agree with those observed by Okai (1981) and by Fujiwara *et al.* (1983), whereas the relations obtained from the experiments of Blaschko *et al.* (1979) are different. Apart from the mechanism proposed by Hyde & O'Keeffe (1973) and Watanabe *et al.* (1977), Okai (1981) introduced a modified Buerger mechanism to explain his experimental results.

Not only the experiments but also theoretical studies led to differing results. Lattice-energy calculations by Nakagiri & Nomura (1982) and molecular dynamics simulations of the phase transition by Ruff *et al.* (1989) favour the transition mechanism proposed by Hyde & O'Keeffe (1973) and Watanabe *et al.* (1977). Applying molecular dynamics studies, Pendás *et al.* (1994) achieved a modified Buerger mechanism, while Nga & Ong (1992) and Sims *et al.* (1998) found that the activation energies of the two mechanisms are very similar.

In a recent work, Sowa & Ahsbahs (1999) studied the pressure-induced phase transition in KPF_6 that leads from an NaCl-related phase to a CsCl-related phase. Since single crystals of the high-pressure modification were obtained, the orientation relations between the two phases could be determined precisely. Irrespective of the fact that CsCl-related KPF_6 exhibits the space group $R\bar{3}$ with a rhombohedral angle of approximately $97°$ instead of $90°$, the phase transition follows the mechanism proposed by Hyde & O'Keeffe (1973) and Watanabe *et al.* (1977). This result stimulated the present study, which aims to give a crystallographic description of this transition mechanism.

2. Symmetry relations between the NaCl and the CsCl types

Fig. 1 shows the relative orientations of the cubic unit cells before and after the phase transition. In order to illustrate the transformation, the processes that occur simultaneously are separated: As shown by Watanabe *et al.* (1977), every other $(001)_{NaCl}$ plane moves parallel to the $[110]_{NaCl}$ direction by $\frac{1}{4}2^{1/2}a_{NaCl}$. This means that the atoms in adjacent planes are shifted by $\frac{1}{8}2^{1/2}a_{NaCl}$ in opposite directions (*cf.* Figs. 2a, 2b). With unchanged metrics, an orthorhombically distorted CsCl-type structure would result. The face diagonal of the unit cell in the $[1\bar{1}0]_{CsCl}$ direction would have a length of $\frac{1}{2}2^{1/2}a_{NaCl}$ and the one in the $[110]_{CsCl}$ direction a length of a_{NaCl}. To achieve equal lengths of both face diagonals, the one parallel to $[1\bar{1}0]_{CsCl} \parallel [1\bar{1}0]_{NaCl}$ has to be elongated while that parallel to $[110]_{CsCl} \parallel [001]_{NaCl}$ must be shortened. Finally, the CsCl-type unit cell has to be contracted along $[00\bar{1}]_{CsCl} \parallel [110]_{NaCl}$ (*cf.* Figs. 2c, 2d). Provided that in fact these structural changes take place simultaneously, each atom adheres to its nearest neighbours while two additional atoms enter the coordination sphere.

The analogous displacements of all atoms and the retention of the nearest neighbours indicate that the structural alterations during the phase transition may be described by means of a sphere-packing deformation. Usually, one assumes that the anions in a crystal structure form the sphere packing while the cations occupy the voids therein. However, in the case of an *AB* compound with the NaCl type where the sizes of the ions are not very different, both kinds of atoms together build up a heterogeneous sphere packing. Since it is much easier to investigate homogeneous sphere packings, the analogous one formed by like atoms is studied. Replacing the atoms in an NaCl-type structure with like atoms results in an arrangement that corresponds to the invariant cubic lattice complex *cP* and to a sphere packing of type 6/4/c1 (Fischer, 1973) with six contacts per sphere. Its space group is $Pm\bar{3}m$ with a lattice parameter *a*, which is half as long as that of $Fm\bar{3}m$. The CsCl-related atomic arrangement of like atoms corresponds to the invariant cubic lattice complex *cI* and to a sphere packing of type 8/4/c1 (Fischer, 1973) with symmetry $Im\bar{3}m$. Starting from $Pm\bar{3}m$, the symmetry has to be reduced until it is possible to deform the sphere packing in the way described above without losing sphere contacts. The resulting space group is a subgroup of both $Pm\bar{3}m$ and $Im\bar{3}m$. When the threefold axes are removed, the translation-equivalent subgroup $P4/mmm$ of $Pm\bar{3}m$ is obtained (Fig. 3). Maintaining the diagonal mirror planes results in the translation-equivalent subgroup $Cmmm$ of $P4/mmm$ with $\mathbf{a}' = \mathbf{a} - \mathbf{b}$, $\mathbf{b}' = \mathbf{a} + \mathbf{b}$, $\mathbf{c}' = \mathbf{c}$. Further symmetry reduction leads to the class-equivalent subgroup $Cmcm$ of $Cmmm$ with doubled *c* lattice parameter. In the standard setting, the origin of the unit cell is shifted by a vector

Figure 1
Stereographic projection showing the orientation relations between the cubic NaCl type and the cubic CsCl type according to the transition model proposed by Hyde & O'Keeffe (1973) and Watanabe *et al.* (1977). Squares: poles of ⟨100⟩ directions of the NaCl type. Circles: poles of ⟨100⟩ and ⟨111⟩ directions of the CsCl type. Dashed lines indicate the ⟨110⟩ and ⟨100⟩ zones of the NaCl type. All poles are on the upper hemisphere.

$(0, 0, -\frac{1}{4})$ relative to that of $Cmmm$ and the cP configuration occurs as a limiting form at position $4(c)$ $m2m$ $0, y, \frac{1}{4}$ with $y = 0$ and $a/b = 1$ and $c/b = 2^{1/2}$. Starting from $Im\bar{3}m$, symmetry reduction results in the intermediate space groups $I4/mmm$ and $Fmmm$. The cI configuration is found in $Cmcm$ with $\mathbf{a}' = \mathbf{a} - \mathbf{b}$, $\mathbf{b}' = -\mathbf{c}$, $\mathbf{c}' = \mathbf{a} + \mathbf{b}$ at position $4(c)$ $m2m$ $0, y, \frac{1}{4}$ with $y = \frac{1}{4}$ and $a/b = c/b = 2^{1/2}$. The origins of the unit cells of $Fmmm$ and $Cmcm$ are shifted against each other by a vector $(0, \frac{1}{4}, \frac{1}{4})$.

The analogous symmetry reduction for NaCl-type structures leads from $Fm\bar{3}m$ via $I4/mmm$ and $Immm$ to $Pmnm$ (nonstandard setting of $Pmmn$). This space group was already stated by Christy (1993) for the intermediate phase produced by the mechanism of Hyde & O'Keeffe (1973) and Watanabe *et al.* (1977). To obtain the undistorted structure, the positions $2(a)$ $m2m$ $0, y, 0$ with $y = \frac{1}{4}$ and $2(b)$ $m2m$ $0, y, \frac{1}{2}$ with $y = \frac{1}{4}$ have to be occupied and $a/b = 1$ and $c/b = 2^{1/2}$ must be fulfilled. The reverse relationship between a CsCl-type and an NaCl-type structure leads from $Pm\bar{3}m$ via $P4/mmm$ and $Cmmm$ to $Pmnm$. If the positions $2(a)$ $m2m$ $0, y, 0$ with $y = 0$ and $2(b)$ $m2m$ $0, y, \frac{1}{2}$ with $y = \frac{1}{2}$ are occupied and $a/b = c/b = 2^{1/2}$ are fulfilled, the ideal CsCl arrangement is obtained. These rela-

tions are described in detail in Fig. 4. To obtain the standard setting $Pmmn$, the unit-cell edges have to be transformed as follows: $\mathbf{a}' = \mathbf{a}$, $\mathbf{b}' = -\mathbf{c}$, $\mathbf{c}' = \mathbf{b}$.

The structural alterations that lead to the phase transitions mentioned above can be studied by examining the possible deformations of sphere packings of type 6/4/c1 within the lattice complex $00\frac{1}{4}\,2_1..\,C_cF1y$ with the characteristic Wyckoff position $Cmcm$ $4(c)$ $m2m$ $0, y, \frac{1}{4}$. This lattice complex has three parameters that may be varied: the positional parameter y and two axial ratios a/b and c/b. Since only little is known so far about sphere configurations with the corresponding symmetry (O'Keeffe & Hyde, 1996), $00\frac{1}{4}\,2_1..\,C_cF1y$ was investigated in the same way as the lattice complex $R6x\bar{x}z$ $[R\bar{3}m\ 18(h)]$ (Sowa & Koch, 1999).

3. Derivation of sphere configurations belonging to $00\frac{1}{4}\,2_1..\,C_cF1y$ [$Cmcm$ 4(c)]

The lattice complex $00\frac{1}{4}\,2_1..\,C_cF1y$ [$Cmcm$ $4(c)$] occurs also in the Wyckoff positions $Pbcn$ $4(c)$, $Pnna$ $4(d)$, $Ama2$ $4(b)$, $Cmc2_1$ $4(a)$ and $C222_1$ $4(a)$ and $4(b)$ (*cf. International Tables for Crystallography*, 1995, Vol. A, ch. 14) and it can be found as a limiting complex in the special positions $Pnnm$ $4(g)$, $Pnma$ $4(c)$ and $Pbcm$ $4(d)$ and also in the general positions of $Pbca$, $Pnn2$, $Pna2_1$, $Pca2_1$, $P2_12_12_1$ and $P2_12_12$ (Engel *et al.*, 1984). Therefore, all sphere configurations that occur in $Cmcm$ $4(c)$ can be found with lower site symmetry in all these space groups.

As pointed out by Fischer (1991*a*) for geometrical investigations of a certain Wyckoff position of a space group G, it is not necessary to consider a parameter region that corresponds to an entire asymmetric unit of G. It is sufficient to confine oneself to one asymmetric unit of the Euclidean normalizer $N_E(G)$ (*cf.* Fischer & Koch, 1983). The Euclidean normalizer $N_E(Cmcm)$ of $Cmcm$ is a supergroup of index 4, namely $Pmmm$ with $\mathbf{a}' = \frac{1}{2}\mathbf{a}$, $\mathbf{b}' = \frac{1}{2}\mathbf{b}$, $\mathbf{c}' = \frac{1}{2}\mathbf{c}$ (*cf. International Tables for Crystallography*, 1995, Vol. A, ch. 15) and for the subsequent investigations of Wyckoff position $4(c)$ $0, y, \frac{1}{4}$ of $Cmcm$ the range $0 \le y \le \frac{1}{4}$ was chosen.

As described in a previous paper (Sowa & Koch, 1999) for lattice complex $R6x\bar{x}z$ [$R\bar{3}m\ 18(h)$], for any reference point lying in the asymmetric unit considered, all symmetrically equivalent points with shortest distances to the first one

Figure 2
Schematic representation of the mechanism of the NaCl to CsCl type transition as proposed by Hyde & O'Keeffe (1973) and Watanabe *et al.* (1977). (*a*) Atomic arrangement in an NaCl-type structure; (*b*) movement of the (001) atomic layers parallel to [110] by $\frac{1}{8}2^{1/2}a$; (*c*) metrical variations, arrows indicate the direction of elongation or contraction; (*d*) CsCl-type structure after the phase transition. Thin lines mark the NaCl-type unit cell, heavy lines that of the CsCl type.

Table 1
Possible neighbouring points with shortest distances to a reference point at $0, y, \frac{1}{4}$ with $0 \leq y \leq \frac{1}{4}$ in $Cmcm$ $4(c)$.

Neighbouring points	Position	Squared distance
A	$0, -y, -\frac{1}{4}$	$d_A^2 = 4y^2 + \frac{1}{4}c^2$
	$0, -y, \frac{3}{4}$	
B	$1, y, \frac{1}{4}$	$d_B^2 = a^2$
	$-1, y, \frac{1}{4}$	
C	$0, y, \frac{5}{4}$	$d_C^2 = c^2$
	$0, y, -\frac{3}{4}$	
D	$\frac{1}{2}, -y+\frac{1}{2}, -\frac{1}{4}$	$d_D^2 = \frac{1}{4}a^2 + 4y^2 - 2y + \frac{1}{4} + \frac{1}{4}c^2$
	$\frac{1}{2}, -y+\frac{1}{2}, \frac{3}{4}$	
	$-\frac{1}{2}, -y+\frac{1}{2}, -\frac{1}{4}$	
	$-\frac{1}{2}, -y+\frac{1}{2}, \frac{3}{4}$	
E	$0, -y+1, -\frac{1}{4}$	$d_E^2 = 4y^2 - 4y + 1 + \frac{1}{4}c^2$
	$0, -y+1, \frac{3}{4}$	
F	$\frac{1}{2}, y+\frac{1}{2}, \frac{1}{4}$	$d_F^2 = \frac{1}{4}a^2 + \frac{1}{4}$
	$\frac{1}{2}, y-\frac{1}{2}, \frac{1}{4}$	
	$-\frac{1}{2}, y+\frac{1}{2}, \frac{1}{4}$	
	$-\frac{1}{2}, y-\frac{1}{2}, \frac{1}{4}$	
G	$0, y+1, \frac{1}{4}$	$d_G^2 = 1$
	$0, y-1, \frac{1}{4}$	

Table 2
Sphere configurations with rod or layer-group symmetry belonging to the lattice complex $00\frac{1}{4} 2_1 \dots C_c F1y$ [$Cmcm$ $4(c)$].

Neighbouring points	Symbol	Description
B, C, G	K	Linear chains
A	K	Zigzag chains
AC	$3^6(1,2)$	Ribbons
F, AE, AG, BC	4^4	Plane layers
D, AB	4^4	Wavy layers
BF, FG, AEG, ACE	3^6	Plane layers
CD, BD	3^6	Wavy layers
ABC	4^4IIa	Double layers
BCD	4^4IV	Double layers

were determined. There are 18 such possible neighbouring points forming five pairs and two sets of four points with equal distances to the reference point. Therefore, seven different kinds of possible neighbour exist, which are designated by the capital letters A to G. Table 1 shows for each of them its position referred to the reference point at $0, y, \frac{1}{4}$ and its squared distance to this point. Since the absolute size of the spheres in a sphere configuration is not important, the lattice parameter b may be arbitrarily set to $b = 1$. Then only a and c have to be varied. Fig. 5 shows the parameter range $0 \leq y \leq \frac{1}{4}$ for different axial ratios a/b and c/b. Each of the two-dimensional subregions in one of the subdiagrams in Figs. 5(a)–(m) is distinguished by exactly one kind of neighbouring point with shortest distance to the reference point and can be labelled by the corresponding capital letter (*cf.* Table 1). Accordingly, the

number of nearest neighbours for any inner point of such a subregion is either two (A, B, C, G) or four (D, F) and the corresponding point configurations only give rise to disconnected sphere configurations. The borders between these subregions, however, may correspond to sphere packings, namely if the symmetry operations for generating the neighbours together with the site symmetry $m2m$ of the reference point generate the space group $Cmcm$. In other cases, only a rod group or a layer group is generated and partial configurations without mutual contact occur. In total, there are 35 different possibilities for generating sphere configurations within the regarded parameter region of $Cmcm$ $4(c)$. Two types of partial configurations with rod-group symmetry and four types with layer-group symmetry were found. In Table 2,

Figure 3
Symmetry relations between the cubic P and I structure types.
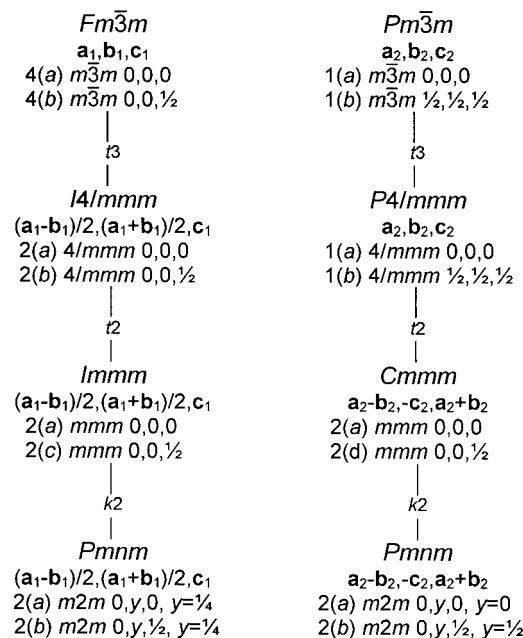
Figure 4
Symmetry relations between the NaCl and the CsCl structure types (same orientation as in Fig. 3). *Pmnm* is a nonstandard setting of *Pmmn*. For the transformation to *Pmnm*, the basis transformation $\mathbf{a}' = \mathbf{a}, \mathbf{b}' = \mathbf{c}, \mathbf{c}' = -\mathbf{b}$ is necessary. The positions $2(a)$ $0,0,z$ with $z = \frac{1}{4}$; $2(b)$ $\frac{1}{2}, 0, z$ with $z = \frac{1}{4}$ (NaCl type); or $2(a)$ $0,0,z$ with $z = 0$; $2(b)$ $\frac{1}{2}, 0, z$ with $z = \frac{1}{2}$ (CsCl type) are occupied.

these sphere configurations are listed. The symbols for rodlike and layerlike configurations were taken from Koch & Fischer (1978). 11 different types of homogeneous sphere packings are generated in *Cmcm* 4(*c*). The sphere packings are listed in

Table 3: They are symbolized according to Fischer (1973, 1974, 1991*a,b*, 1993) and Koch & Fischer (1995). Each sphere-packing type is designated by a symbol *k/m/fn*: *k* means the number of contacts per sphere, *m* is the size of the shortest
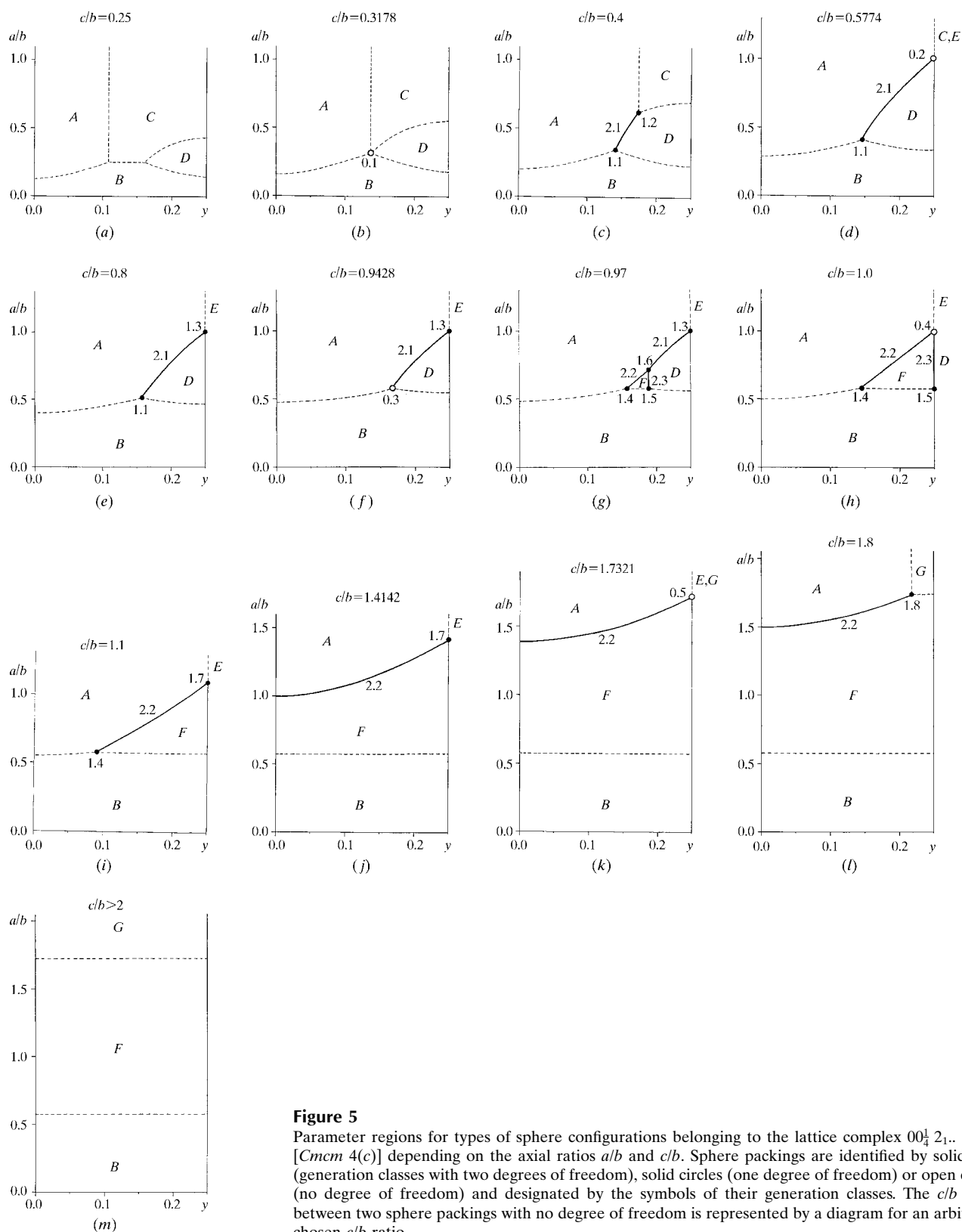
Figure 5
Parameter regions for types of sphere configurations belonging to the lattice complex $00\frac{1}{4}$ 2_1.. C_cF1y [*Cmcm* 4(*c*)] depending on the axial ratios *a/b* and *c/b*. Sphere packings are identified by solid lines (generation classes with two degrees of freedom), solid circles (one degree of freedom) or open circles (no degree of freedom) and designated by the symbols of their generation classes. The *c/b* range between two sphere packings with no degree of freedom is represented by a diagram for an arbitrarily chosen *c/b* ratio.

Table 3
Sphere-packing conditions for $00\frac{1}{4}2_1C_c..$ $F1y$ [$Cmcm$ $4(c)$].

Sphere-packing type	Generation class	Neighbouring points	Sphere-packing conditions			
6/4/h2	2.1	AD	$\frac{1}{4}a^2 - 2y + \frac{1}{4} = 0$			
6/4/c1	2.2	AF	$\frac{1}{4}a^2 - 4y^2 + \frac{1}{4} - \frac{1}{4}c^2 = 0$			
8/4/c1	2.3	DF	$4y^2 - 2y + \frac{1}{4}c^2 = 0$			
8/3/o1	1.1	ABD	2.1	$a^2 - 4y^2 - \frac{1}{4}c^2 = 0$		
8/3/h3	1.2	ACD	2.1	$y = \frac{1}{4}3^{1/2}c$		
8/4/c1	1.3	ADE	$a = 1$	$y = \frac{1}{4}$		
8/3/h4	1.4	ABF	$a = \frac{1}{3}3^{1/2}$	$y = \frac{1}{2}(\frac{1}{3} - \frac{1}{4}c^2)^{1/2}$		
10/3/t1	1.5	BDF	2.3	$a = \frac{1}{3}3^{1/2}$		
10/3/o1	1.6	ADF	2.1	2.2		
8/4/c1	1.7	AEF	$a = c$	$y = \frac{1}{4}$		
8/3/h4	1.8	AFG	$a = 3^{1/2}$	$y = \frac{1}{2}(1 - \frac{1}{4}c^2)^{1/2}$		
10/3/o2	0.1	ABCD	$y = 0.1376$	$a = 1/(2^{1/2} + 3^{1/2})$	$c = 1/(2^{1/2} + 3^{1/2})$	$\rho = 66.6\%$
10/3/t1	0.2	ACDE	$y = \frac{1}{4}$	$a = 1$	$c = \frac{1}{3}3^{1/2}$	$\rho = 69.8\%$
12/3/h1	0.3	ABDF	$y = \frac{1}{6}$	$a = \frac{1}{3}3^{1/2}$	$c = \frac{2}{3}2^{1/2}$	$\rho = 74.1\%$
12/3/c1	0.4	ADEF	$y = \frac{1}{4}$	$a = 1$	$c = 1$	$\rho = 74.1\%$
10/3/t1	0.5	AEFG	$y = \frac{1}{4}$	$a = 3^{1/2}$	$c = 3^{1/2}$	$\rho = 69.8\%$

mesh, f indicates the highest crystal family for sphere packings of that type and n is an arbitrary number. In the second column, the generation class is given, which is designated by a symbol $g.h$ (Fischer, 1991a), where g gives the number of degrees of freedom and h is an arbitrary number. The third

Figure 6
Variations of the normalized lattice parameters (shortest interatomic distance $d = 1$) depending on the positional parameter y during the transformation from the NaCl type to the CsCl type according to the mechanism proposed by Hyde & O'Keeffe (1973) and Watanabe *et al.* (1977): (*a*) in a transition model with $c/b = 2^{1/2}$; (*b*) in a model with six equal distances to the next-nearest neighbours during the transition.

column of Table 3 shows the nearest neighbours of the reference point. In the fourth column, the sphere-packing conditions that must be fulfilled by the positional parameters of the sphere centres and by the metrical parameters of the unit cell are listed. Referring to a lattice parameter $b = 1$, only the parameters a, c and y are needed in these equations. For all sphere packings with fixed parameters, the y coordinate of the centre of the reference sphere, the a and c parameters, and the space filling ρ are listed.

In three generation classes, sphere-packing types with two degrees of freedom occur, in eight classes those with one, and in five classes those with no degree of freedom. As may be read from their symbols, sphere packings of the types 6/4/c1, 6/4/h2, 8/4/c1, 8/3/h3, 8/3/h4, 10/3/t1, 12/3/h1 and 12/3/c1 may also occur with higher symmetry because the orthorhombic lattice complex $00\frac{1}{4}2_1.. C_cF1y$ [$Cmcm$ $4(c)$] comprises the corresponding cubic, hexagonal and tetragonal lattice complexes as limiting forms (*cf.* Table 4). Both orthorhombic sphere packings with ten contacts per sphere have already been noted before: 10/3/o1 is described by O'Keeffe & Hyde (1996) and information on 10/3/o2 can be found in *International Tables for Crystallography* (1992), Vol. C, ch. 9.

4. Description of the $cP \rightarrow cI$-type phase transition

A sphere packing that may be deformed in such a way that a transition from a cP to a cI configuration results is of type 6/4/c1 and belongs to the generation class 2.2. The corresponding sphere-packing condition is

$$y = \frac{1}{4}[(a/b)^2 - (c/b)^2 + 1]^{1/2}. \tag{1}$$

Its two-dimensional parameter region is bounded by those of the sphere-packing types with one degree of freedom belonging to the generation classes 1.4, 1.6, 1.7 and 1.8 and by the parameters of the sphere-packing types with no degree of freedom belonging to the classes 0.3, 0.4 and 0.5 (*cf.* Figs. 5*f–m*). The ideal cubic *P* configuration occurs at $y = 0$, $a/b = 1$ and $c/b = 2^{1/2}$. In the case of like atoms, deformations leading
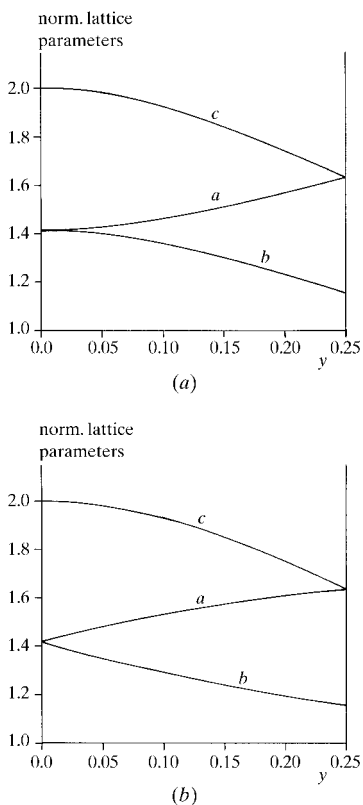
to each of these more dense sphere packings are conceivable. For instance, without losing sphere contacts, a cP configuration may be deformed into a configuration that can be described with a sphere packing of type $8/3/h4$ (generation class 1.8). Such atomic arrangements can be observed in the high-pressure phases of silicon and germanium (see below). Also, hexagonal $12/3/h1$ (0.3) or cubic close packings $12/3/c1$ (0.4) may be obtained. Both deformations, however, are not possible in crystals with NaCl-type structures because such crystals contain two kinds of ions. In these cases, atoms labelled B, C, D and G denote like atoms while A, E and F represent unlike atoms referred to the reference atom. Therefore, the only sphere packings with higher contact number that may be reached belong to type $8/4/c1$ (1.7). This type has one degree of freedom and the ideal cubic body-centred arrangement is found at $y = \frac{1}{4}$, $a/b = c/b = 2^{1/2}$.

The question arises: what is the transition path from the cP (NaCl)-type to the cI (CsCl)-type configuration? The true path cannot be determined geometrically but may be found by employing energetic calculations throughout the parameter region of 2.2. Two conceivable paths are represented:

(i) Not only in the NaCl type but also in the CsCl type the ratio c/b is $2^{1/12}$. Therefore, it may be suggested that the b and c unit-cell parameters shorten synchronously leaving the c/b ratio constant. In this case, y depends only on a/b and equation (1) is reduced to

$$y = \tfrac{1}{4}[(a/b)^2 - 1]^{1/2}. \qquad (2)$$

Fig. 6(a) shows the variation of the unit-cell parameters depending on y for a model with six nearest neighbours at a distance of $d = 1$ and $c/b = 2^{1/2}$. The corresponding normalized interatomic distances are shown in Fig. 7(a).

(ii) The second transition path that may be suggested assumes that six of the next-nearest neighbours keep equal distances to the reference atom during the transformation. This model should be electrostatically more favourable than the first one. The geometrical condition for such a transformation is

$$c/b = (2 + 4y - 16y^2)^{1/2}. \quad (3)$$

Fig. 6(b) shows the variations of the the unit-cell parameters and Fig. 7(b) the normalized distances for such a transformation. For comparison, the corresponding interatomic distances during the transition that corresponds to the mechanism proposed by Buerger (1951) are given in Fig. 7(c). Figs. 7(a)–(c) show that the atomic distances in the close vicinity of each atom are very similar in all these cases. Possibly this is the reason why the two different mechanisms are energetically similar. Differences could only be seen by looking at more distant neighbours. For instance, the 12 atoms of the third coordination shell in the CsCl type partly originate from different neighbours in the NaCl type. Six of
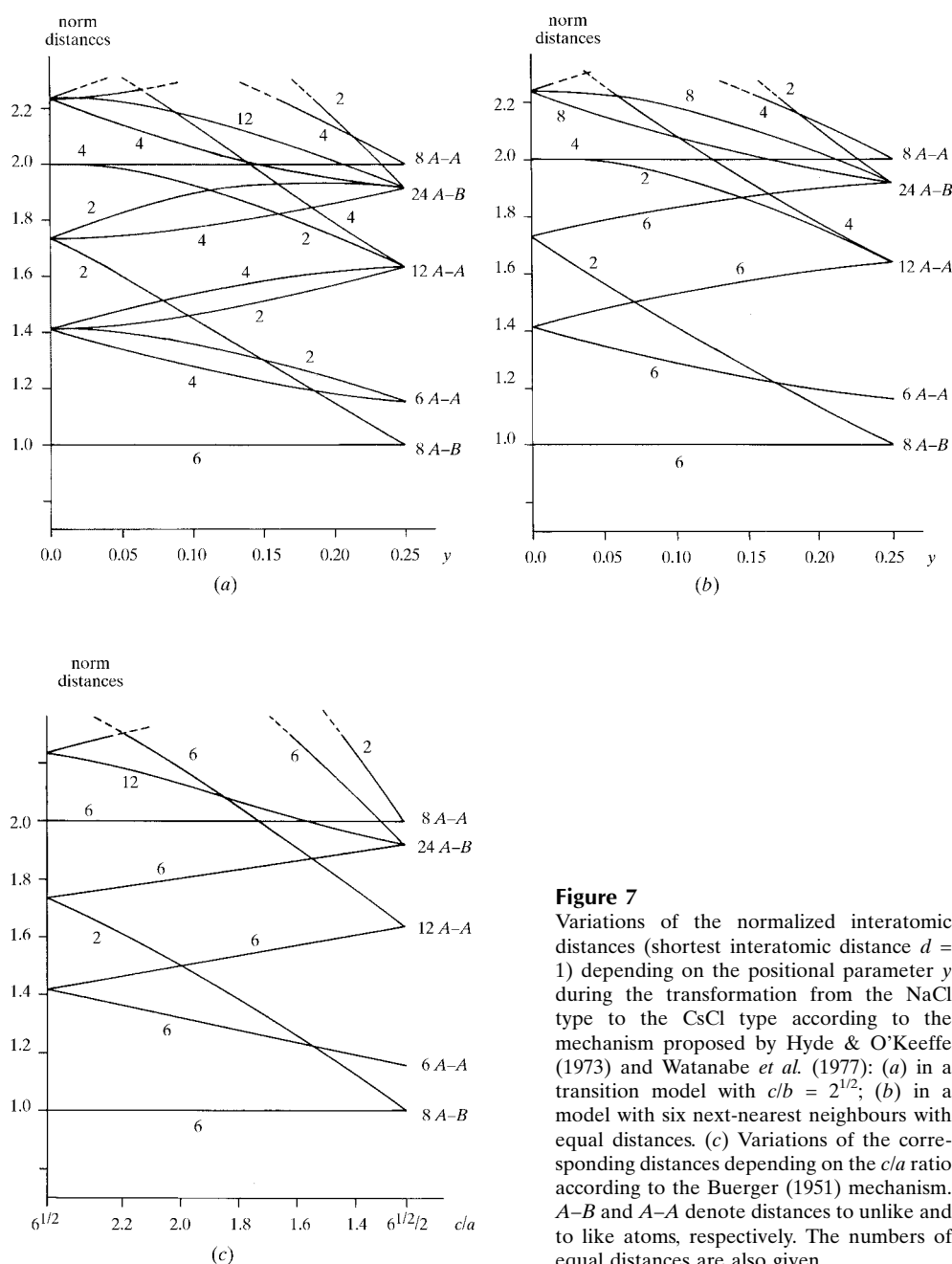
Figure 7
Variations of the normalized interatomic distances (shortest interatomic distance $d = 1$) depending on the positional parameter y during the transformation from the NaCl type to the CsCl type according to the mechanism proposed by Hyde & O'Keeffe (1973) and Watanabe *et al.* (1977): (a) in a transition model with $c/b = 2^{1/2}$; (b) in a model with six next-nearest neighbours with equal distances. (c) Variations of the corresponding distances depending on the c/a ratio according to the Buerger (1951) mechanism. A–B and A–A denote distances to unlike and to like atoms, respectively. The numbers of equal distances are also given.

Table 4
Limiting forms of cubic, tetragonal and hexagonal lattice complexes and sphere-packing types belonging to $Cmcm$ $4(c)$ with $b = 1$.

Lattice complex	Characteristic Wyckoff position	Sphere-packing type	Generation class	Positional and metrical parameters		
cI	$Im\bar{3}m$ $2(a)$	$8/4/c1$	1.7	$y = \frac{1}{4}$	$a = 2^{1/2}$	$c = 2^{1/2}$
		$8/4/c1$	1.3	$y = \frac{1}{4}$	$a = 1$	$c = \frac{1}{2}2^{1/2}$
		$8/4/c1$	2.3	$y = \frac{1}{4}$	$a = \frac{1}{2}2^{1/2}$	$c = 1$
cF	$Fm\bar{3}m$ $4(a)$	$12/3/c1$	0.4	$y = \frac{1}{4}$	$a = 1$	$c = 1$
cP	$Pm\bar{3}m$ $1(a)$	$6/4/c1$	2.2	$y = 0$	$a = 1$	$c = 2^{1/2}$
E	$P6_3/mmc$ $2(c)$	$12/3/h1$	0.3	$y = \frac{1}{6}$	$a = \frac{1}{3}3^{1/2}$	$c = \frac{2}{9}2^{1/2}$
		$8/3/h3$	1.2	$y = \frac{1}{6}$	$a = \frac{1}{3}3^{1/2}$	$c = \frac{2}{3}3^{1/2}$
		$6/4/h2$	2.1	$y = \frac{1}{6}$	$a = \frac{1}{3}3^{1/2}$	$\frac{2}{9}3^{1/2} < c < \frac{2}{3}2^{1/2}$
hP	$P6/mmm$ $1(a)$	$8/3/h4$	1.4	$y = 0$	$a = \frac{1}{3}3^{1/2}$	$c = \frac{2}{3}3^{1/2}$
		$8/3/h4$	1.8	$y = 0$	$a = 3^{1/2}$	$c = 2$
tI	$I4/mmm$ $2(a)$	$10/3/t1$	1.5	$y = \frac{1}{4}$	$a = \frac{1}{3}3^{1/2}$	$c = 1$
		$10/3/t1$	0.2	$y = \frac{1}{4}$	$a = 1$	$c = \frac{1}{3}3^{1/2}$
		$10/3/t1$	0.5	$y = \frac{1}{4}$	$a = 3^{1/2}$	$c = 3^{1/2}$

these neighbours belong to the second coordination shell in the NaCl type. According to the mechanism proposed by Buerger (1951), during the transition with symmetry $R\bar{3}m$ six further neighbours from the sixth coordination shell of the NaCl type with $d = 2.445$ complete the third shell in the CsCl type. The transition mechanism with symmetry $Pmmn$, however, requires only four neighbours of the sixth coordination shell of the NaCl type with $d = 2.445$, whereas the other two originate from the fourth shell with $d = 2.0$ of the NaCl type (cf. Figs. 7a–c). Unfortunately, these graphical illustrations may obscure the fact that the comparable distances belong to different atoms for the mechanisms proposed by Buerger (1951) and by Hyde & O'Keeffe (1973) and Watanabe et al. (1977). As Fig. 8 shows, the two neighbours that join the first coordination sphere of the central ion are different in the two cases. Since the absolute atomic shifts in the model of Buerger (1951) are larger than in that of Hyde & O'Keeffe (1973) and Watanabe et al. (1977), the latter mechanism is possibly favoured.

Using the mechanism of Hyde & O'Keeffe (1973) and Watanabe et al. (1977), the orthorhombic b and c parameters would shrink by about 18% while a would expand by about 15% if the nearest distances between the anions and cations do not change during the transition from the NaCl to the CsCl type. Whereas for like atoms such alterations may be possible, in the case of unlike atoms it must be kept in mind that the distances to the next-nearest neighbours in CsCl-type crystal structures are only about 15% longer than the nearest ones. Thus, if the distances between the cations and the anions were constant, the shortest distances between equal charged ions would be too short. For instance, in NaCl they would be shorter than twice the anion radius. Therefore, the repulsions between the equally charged ions cause an elongation of the shortest distances between cations and anions. Such an effect would occur in any case independent of the transition mechanism.

Phase transitions in ionic compounds proceed very rapidly so that the intermediate phase cannot be observed. However, both possible intermediate structure types are realized in some substances. For instance, a rhombohedrally distorted

NaCl-type structure may be stabilized by hydrogen bonds as occur in hydrogen sulfides of alkali metals (Jacobs et al., 1991). At low temperatures, CrN undergoes a phase transition from a cubic NaCl-type structure into a slightly orthorhombically distorted variant with symmetry $Pmmn$ (Eddine et al., 1969). It

(a)

(b)
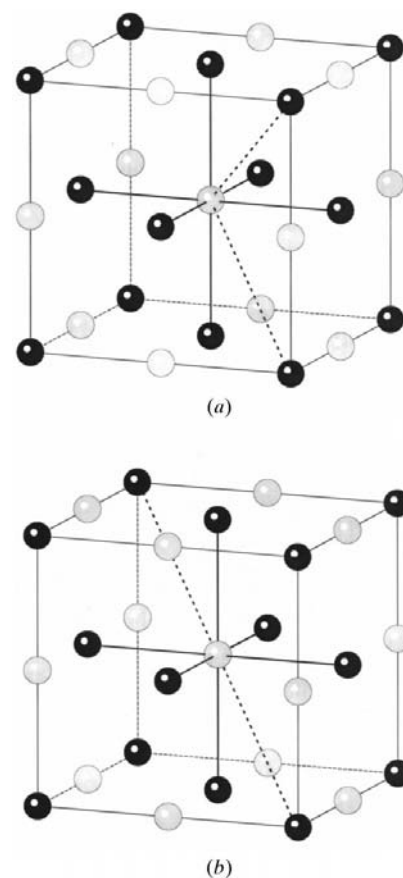
Figure 8
Unit cell of an NaCl-type structure. Bold lines indicate the six nearest neighbours, dashed lines direct to the additional neighbours in a CsCl-type structure according to the mechanisms proposed by (a) Hyde & O'Keeffe (1973) and Watanabe et al. (1977) and (b) Buerger (1951).

is also conceivable that such structures exist in covalently bonded compounds under high pressure too.

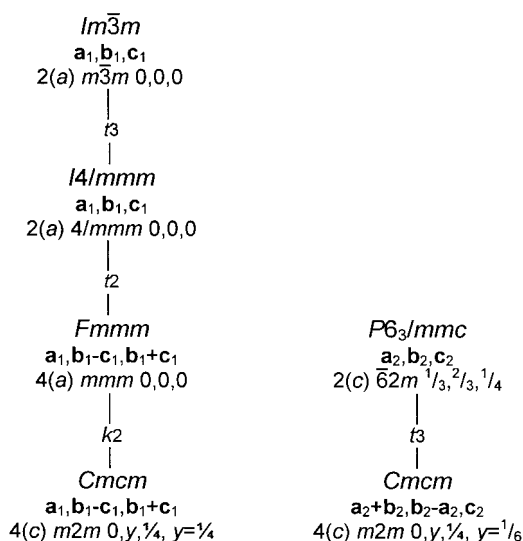## 5. Other structural examples for sphere packings in *Cmcm* 4(*c*)

On inspection of the sphere configurations that may be generated with the symmetry *Cmcm* 4(*c*), it becomes obvious that not only the deformation from a *cP* configuration into a *cI* configuration is possible. Two further types of phase transitions that may occur in metal structures can also be described.

5.1. *cI* → h.c.p.

Sphere packings of type 8/4/c1 belonging to the generation class 2.3 in *Cmcm* 4(*c*) have two degrees of freedom. The ideal *cI* configuration is found at $y = \frac{1}{4}$, $a/b = \frac{1}{2}2^{1/2}$ and $c/b = 1$. It may be deformed into a hexagonal close packing (h.c.p.) that is reached at $y = \frac{1}{6}$, $a/b = \frac{1}{3}3^{1/3}$ and $c/b = \frac{2}{3}2^{1/2} \simeq 0.9428$ (generation class 0.3). The sphere-packing condition is

$$y = \tfrac{1}{4} - \tfrac{1}{4}[1 - (c/b)^2]^{1/2}. \qquad (4)$$

Such a transition is accompanied by the increase of the coordination number from eight to twelve. The hexagonal close packing occurs with the highest symmetry in $P6_3/mmc$, which is a minimal supergroup of *Cmcm*. The group–subgroup relations are shown in Fig. 9. Such a transformation occurs in barium at high pressures while in zirconium the reverse transformation takes place at high temperatures. Both transitions were investigated by first-principles calculations by Ye *et al.* (1987) and Chen *et al.* (1988) and the results were summarized by Harmon (1994). The geometrical relations between a body-centred cubic (b.c.c.) and a hexagonal close-packed structure (h.c.p.) have already been analysed by Burgers (1934), who derived that $(110)_{bcc}$ is parallel to $(001)_{hcp}$

and $[111]_{bcc}$ is parallel to $[110]_{hcp}$. Fig. 10 shows the corresponding atomic movements.

The transition path is described by Harmon (1994) but without any symmetry information. He states that during the transformation the angle Θ (*cf.* Fig. 10) varies from 109.4 to 120°. This yields a probable transition path if one assumes that four of the next-nearest-neighbouring atoms retain equal distances. In this case, the additional condition

$$a/b = (2y)^{1/2} \qquad (5)$$

is required. Fig. 11 shows for this transition the variations of the unit-cell parameters with nearest interatomic distances of
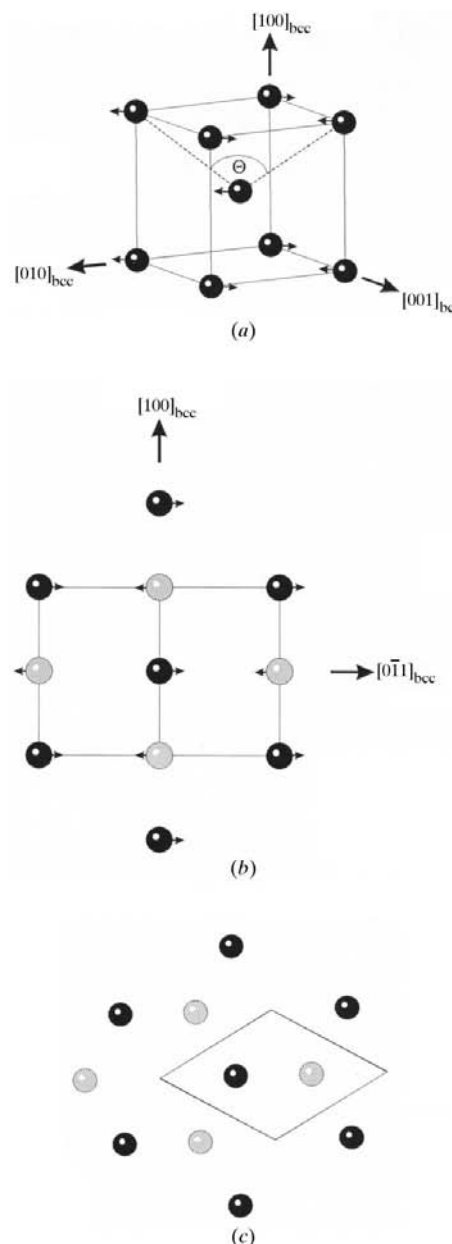
Figure 10
(*a*) Transformation from the *cI* type to a hexagonal close packing. (*b*) Projection parallel to $[011]_{bcc}$. Arrows indicate the direction of the atomic shifts. (*c*) Projection parallel to $[001]_{hcp}$. Different shadings indicate atoms at different heights. Thin lines mark the respective unit cells.

Figure 9
Symmetry relations between a structure of the *cI* type and a hexagonal close-packed structure

$d = 1$ and Fig. 12 shows the corresponding interatomic distances *versus* y. During the deformation, the cubic body-centred unit cell is shortened in the [100] direction while in the [0$\bar{1}$1] direction it is elongated (*cf.* Fig. 10). As noted by Harmon (1994), who used the *c/a* ratio of the deformed h.c.p. structure, the orthorhombic *c* parameter that has the same value in the *cI*-type structure and in the hexagonally close packed configuration varies during the transformation (*cf.* Fig. 11).

5.2. *ph* → h.c.p.

Another type of transformation that may be described by means of sphere packings is the transition between a primitive hexagonal crystal structure (*ph*) with coordination number eight that occurs as a high-pressure modification of silicon and germanium (*e.g.* Olijnyk *et al.*, 1984) and a hexagonal close-packed structure. The corresponding phase transformation was supposed to take place in silicon. It was investigated by Chang & Cohen (1985) by employing *ab initio* pseudopotential calculations. The authors state that during the transition the (001) planes are shifted by $a/3^{1/2}$ with respect to the neighbouring ones along the [110] direction of the hexagonal cell. However, a figure given in the paper shows that [210] is meant.

The primitive hexagonal structures form sphere packings of type 8/3/h4 that can be found with highest symmetry in $P6/mmm$ with $c/a = 1$ at position 1(*a*) 6/*mmm* 0,0,0. In *Cmcm* 4(*c*), sphere packings of this type occur with one degree of freedom (1.4). The corresponding sphere-packing conditions are

$$a/b = \tfrac{1}{3}3^{1/2} \quad \text{and} \quad y = \tfrac{1}{2}[\tfrac{1}{3} - \tfrac{1}{4}(c/b)^2]^{1/2}. \tag{6}$$

The undistorted arrangement exists at $y = 0$, $a/b = \tfrac{1}{3}3^{1/2}$ and $c/b = \tfrac{2}{3}3^{1/2} \simeq 1.1547$. It can be deformed without losing contacts until a hexagonal close packing (0.3) with inherent symmetry $P6_3/mmc$ 2(*c*) is reached at $y = \tfrac{1}{6}$, $a/b = \tfrac{1}{3}3^{1/2}$ and $c/b = \tfrac{2}{3}2^{1/2} \simeq 0.9428$.
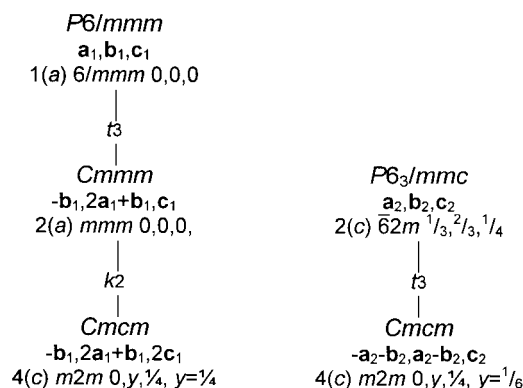
Fig. 13 shows the relations between *Cmcm* and its two supergroups $P6/mmm$ and $P6_3/mmc$. During the phase transition, the atoms in adjacent (001) planes of the 8/3/h4 arrangement are shifted in opposite directions by $\tfrac{1}{6}3^{1/2}a$ against each other along the [210] direction of the hexagonal
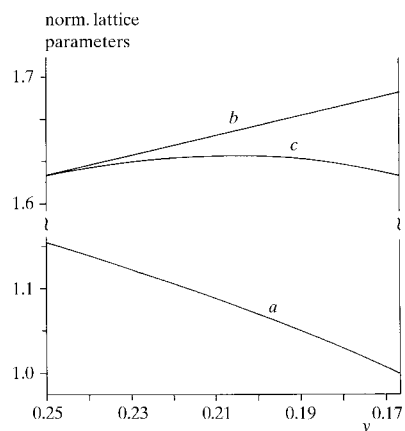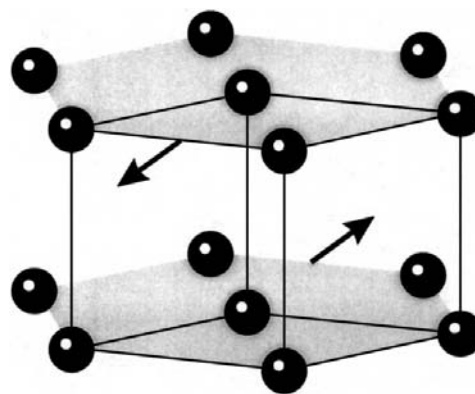

Figure 11
Variations of the normalized lattice parameters (shortest interatomic distance $d = 1$) depending on the positional parameter y during the transformation from the *cI* type to a hexagonal close packing.

Figure 13
Symmetry relations between a primitive hexagonal structure and a hexagonal close-packed structure.

Figure 12
Variations of the normalized interatomic distances (shortest interatomic distance $d = 1$) depending on the positional parameter y during the transformation from the *cI* type to a hexagonal close packing.
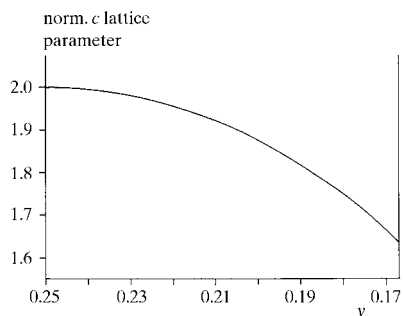

Figure 14
Transformation from a primitive hexagonal structure to a hexagonal close packing. Arrows indicate the direction of the shifts of the atomic planes.

cell (Fig. 14). If the distances of the nearest neighbours are maintained, the a and b lattice parameters of $Cmcm$ remain constant while c decreases. Fig. 15 shows the variation of c for a sphere packing of type $8/3/h4$ in $Cmcm$ $4(c)$ with shortest interatomic distances of $d = 1$ depending on the y parameter. Fig. 16 displays the corresponding interatomic distances *versus* y.

Recent work on the high-pressure behaviour of silicon (Hanfland *et al.*, 1999) revealed, however, that such a transition mechanism does not take place in this substance. The intermediate phase between the hexagonal primitive phase with a coordination number of eight for all atoms and the twelvefold-coordinated hexagonal-close-packed phase is the Si-VI phase. Its more complicated structure is found to be orthorhombic with space group $Cmca$. Nevertheless, it is possible that the transition from a primitive hexagonal to a hexagonal-close-packed structure as described above may take place in other substances.

5.3. $cI \rightarrow cF$

In $Cmcm$ $4(c)$, this deformation that leads from a cubic body-centred configuration to a cubic close packing is realized three times. Sphere packings of type $8/4/c1$ belonging to the generation classes 2.3, 1.3 and 1.7 may be deformed without losing contacts to sphere packings of type $12/3/c1$ (0.4). However, such transformations that have been observed in many metals at high pressures or the reverse transitions that may occur at high temperatures can be described with higher symmetry in $I4/mmm$ at position $2(a)$ $0,0,0$.

6. Conclusions

Sphere packings are not only a useful tool for describing the crystal structures of many relatively simple compounds (O'Keeffe & Hyde, 1996; and references in Sowa & Koch, 1999). Although the atomic arrangements in real compounds show deviations from ideal sphere packings, deformations of sphere packings can be used to imagine phase transitions that possibly may occur depending on pressure or on temperature. The geometric aspects of such a displacive phase transition and their crystallographic description can be analysed by investigating the possible deformations of the sphere packing in question. Details concerning the deviations from the ideal case may be interpreted by employing energetic calculations.

Figure 15
Variation of the normalized lattice parameter c (shortest interatomic distance $d = 1$) depending on the positional parameter y during the transformation from a primitive hexagonal structure to a hexagonal close packing.
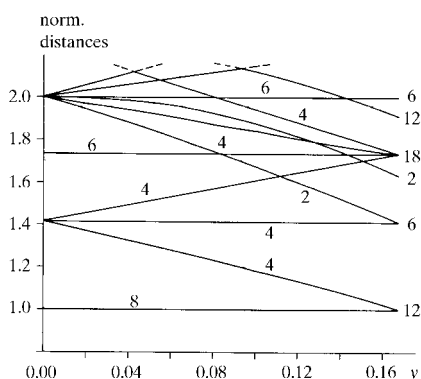
Figure 16
Variations of the normalized interatomic distances (shortest interatomic distance $d = 1$) depending on the positional parameter y during the transformation from a primitive hexagonal structure to a hexagonal close packing.

References

Blaschko, O., Ernst, G., Quittner, G., Pépy, G. & Roth, M. (1979). *Phys. Rev. B*, **20**, 1157–1163.
Buerger, M. J. (1951). *Phase Transformations in Solids*, edited by R. Smoluchowski, J. E. Mayers & W. A. Weyl, pp. 183–211. New York: John Wiley.
Burgers, W. G. (1934). *Physica (Utrecht)*, **1**, 561–586.
Chang, K. J. & Cohen, M. L. (1985). *Phys. Rev. B*, **31**, 7819–7826.
Chen, Y., Ho, K. M. & Harmon, B. N. (1988). *Phys. Rev. B*, **37**, 283–288.
Christy, A. G. (1993). *Acta Cryst.* B**49**, 987–996.
Eddine, M. N., Sayetat, F. & Bertaut, E. F. (1969). *C. R. Acad. Sci. Ser. B*, **269**, 574–577.
Engel, P., Matsumoto, T., Steinmann, G. & Wondratschek, H. (1984). *Z. Kristallogr.* Suppl. 1.
Fischer, W. (1973). *Z. Kristallogr.* **138**, 129–146.
Fischer, W. (1974). *Z. Kristallogr.* **140**, 50–74.
Fischer, W. (1991*a*). *Z. Kristallogr.* **194**, 67–85.
Fischer, W. (1991*b*). *Z. Kristallogr.* **194**, 87–110.
Fischer, W. (1993). *Z. Kristallogr.* **205**, 9–26.
Fischer, W. & Koch, E. (1983). *Acta Cryst.* A**39**, 907–915.
Fujiwara, H., Nakagiri, N. & Nomura, M. (1983). *J. Phys. Soc. Jpn*, **52**, 1665–1668.
Hanfland, M., Schwarz, U., Syassen, K. & Takemura, K. (1999). *Phys. Rev. Lett.* **82**, 1197–1200.
Harmon, B. N. (1994). *Statics and Dynamics of Alloy Phase Transformations*, edited by P. E. A. Turchi & A. Gonis. *NATO ASI Series, Series B: Physics.* Vol. 319, pp. 421–434.
Hyde, B. G. & O'Keeffe, M. (1973). *Phase Transitions*, edited by L. E. Cross, pp. 345–349. Oxford: Pergamon Press.
International Tables for Crystallography (1992). Vol. C, edited by A. J. C. Wilson. Dordrecht: Kluwer Academic Publishers.
International Tables for Crystallography (1995). Vol. A, edited by Th. Hahn. Dordrecht: Kluwer Academic Publisher.

Jacobs, H., Metzner, U., Kirchgässner, R., Lutz, H. D. & Beckenkamp, K. (1991). *Z. Anorg. Allg. Chem.* **598/599**, 175–192.

Kennedy, S. W. (1980). *J. Solid State Chem.* **34**, 31–37.

Koch, E. & Fischer, W. (1978). *Z. Kristallogr.* **148**, 107–152.

Koch, E. & Fischer, W. (1995). *Z. Kristallogr.* **210**, 407–414.

Nakagiri, N. & Nomura, M. (1982). *J. Phys. Soc. Jpn*, **51**, 2412–2418.

Nga, Y. A. & Ong, C. K. (1992). *Phys. Rev. B*, **46**, 10547–10553.

Okai, B. (1980). *J. Phys. Soc. Jpn*, **48**, 514–519.

Okai, B. (1981). *J. Phys. Soc. Jpn*, **50**, 3189–3190.

O'Keeffe, M. & Hyde, B. G. (1996). *Crystal Structures. I. Patterns and Symmetry.* Washington: Mineralogical Society of America.

Olijnyk, H., Sikka, S. K. & Holzapfel, W. B. (1984). *Phys. Lett.* **103**A, 137–140.

Onodera, A., Nakai, Y., Kawano, S. & Achiwa, N. (1992). *High Temp. High Press.* **24**, 55–63.

Pendás, A. M., Luaña, V., Recio, J. M., Flórez, M., Francisco, E., Blanco, M. A. & Kantorovich, L. N. (1994). *Phys. Rev. B*, **49**, 3066–3074.

Ruff, I., Baranyai, A., Spohr, E. & Heinzinger, K. (1989). *J. Chem. Phys.* **91**, 3148–3159.

Shoji, H. (1931). *Z. Kristallogr.* **77**, 381–410.

Sims, C. E., Barrera, G. D., Allan, N. L. & Mackrodt, W. C. (1998). *Phys. Rev. B*, **57**, 11164–11172.

Sowa, H. & Ahsbahs, H. (1999). *Z. Kristallogr.* **214**, 751–757.

Sowa, H. & Koch, E. (1999). *Z. Kristallogr.* **214**, 316–323.

Watanabe, M., Tokonami, M. & Morimoto, N. (1977). *Acta Cryst.* A**33**, 294–298.

Ye, Y.-Y., Chen, Y., Ho, K. M., Harmon, B. N. & Lindgård, P.-A. (1987). *Phys. Rev. Lett.* **58**, 1769–1772.